



Linking health impact and Post-environmental impact assessments: a case of municipal sewage treatment plant volatile organic compounds

Hongmei Wang¹ · Huifeng Wang² · Ci Zhao³ · Zhanlu Lv¹ · Xiang Huang³ · Xiaoyu Liu³

Received: 11 January 2020 / Accepted: 12 February 2020 / Published online: 2 March 2020
© Springer Nature B.V. 2020

Abstract

Deficiencies remain in current health impact assessment (HIA) and environmental impact assessment (EIA) projects. To address the shortcomings in EIA theory, a case of odors from a municipal sewage treatment plant (MSTP) was examined and geographic factors were employed to associate the spatial diffusion of the pollutants with the population's activities based on land-use attributes. After screening the MSTP priority control pollutants, odors, hydrogen sulfide, and ammonia were selected for this study. Then, the spatial parameters for the pollutant simulation were surveyed, including parameters concerning the meteorological analysis, environmental emission monitoring, and emission source analysis, and a prediction of the pollutant diffusion as imaged and identified. The types of human social activity and exposure patterns were sorted as land-use attributes. An integration of the spatial diffusion of the pollutants with the exposure profiles of the scenario population according to the land-use attributes was achieved using counterpart spatial coordination factors. In our study, the *commonly applied* method of HIA risk calculation was followed and then extended by the spatial techniques introduced. The results of the scenario HIA contours are presented here, making it easy to determine the acceptable levels of the MSTP odor pollutants on a geographic scale. This study examines a significant approach to associate HIA with post-EIA via spatial factors and addresses the deficiencies of HIA in EIA empirical applications.

Keywords Health impact assessment (HIA) · Spatial factor linkage · Environmental impact assessment of operational projects (post-EIA) · Odors · Municipal sewage treatment plant (MSTP)

Highlights

An approach integrating health impact assessment (HIA) and environmental impact assessment (post-EIA) is developed.
A pollutant diffusion simulation is linked to a scenario population's exposure parameters assigned to land-use attributes.

✉ Hongmei Wang
wanghmj@163.com

¹ State Key Laboratory of Environmental Criteria and Risk Assessment & Department of Environment and Health, Chinese Research Academy of Environmental Sciences, Beijing 100012, People's Republic of China

² Department of Technology Development, Chinese Research Academy of Environmental Sciences, Beijing 100012, People's Republic of China

³ Environmental Policy and Strategic Environmental Assessment Research Center, Chinese research academy of environmental sciences, Beijing 100012, People's Republic of China

Introduction

A health impact assessment (HIA) is a process to estimate the nature and probability of adverse health effects in humans who may be exposed to chemicals in contaminated environmental media, now or in the future. Protecting human health from the risk of pollutant exposure is the ultimate goal of environmental protection. Even though environmental impact assessment (EIA) has been a proven tool over the past 35 years and has a good track record in evaluating the environmental risks and opportunities of project proposals and improving the quality of outcomes, its theory and practice for HIA continues to lag behind policy expectations (Lebret 2015; Rouéle and Jabot 2018). China has experienced a worsening environmental situation in recent years due to rapid industrialization (Niu et al. 2017; Lamoreaux and Arizona 2019). While HIA is a part of the EIA system, as claimed by the *China Act Environmental Impact Assessment (revised edition, 2018)*,

a theory integrating HIA into EIA is still under development and remains inadequate in practice (Chang et al. 2017). Most local administrative requirements for HIA in project planning EIA are relatively weak and may even be thoroughly ignorant of environmental decision-making, therefore making them disconnected from HIA in practice.

There is increasing interest in merging HIA into an operational project EIA (post-EIA), which is important for decision-making when planning surrounding land-use and the regulation of protection polices for nearby populations. However, the key technology for merging HIA into EIA is still a challenge and most HIA studies have focused on the accuracy of risk assessments in toxicology and epidemiology (Ruby et al. 1999, Bari and Kindzierski 2018a, b), while there has been little focus on concepts linked to spatial factors. The area impacted by an operational project is defined by its geographic location and the emission intensity, as well as the likely level of exposure, which is associated with the spatial dispersion concentration and the population's exposure patterns. Therefore, more scientific techniques are expected to be introduced into the theory of EIA. With insights into exposure assessments, more scientists are beginning to associate population exposure profiles on a geographic scale with the diffusion of pollutants (Wang et al. 2018a). A geographic information system (GIS) provides a perfect solution to overcome the obstacle of a scenario population's exposure profiles based on the population's social characteristics and the spatial distribution of the pollutants (Vu et al. 2013; Minolfi et al. 2018), which forms a linkage for an HIA scenario based on land use to a post-EIA via counterpart spatial analysis. Several similar studies on how to conduct an HIA have been outlined, some of which are inspiring (Aliyu et al. 2014; Boudet et al. 1999; Spickett et al. 2012; Lei and Hilton 2012; Lebret 2015). Of these, one study was on the health risk assessment of a modern municipal waste incinerator that proposed linking an air pollutant dispersion model to the exposure parameters using the demographic characteristics of the nearby population Boudet et al. 1999). Other studies have attempted to incorporate wind flow effects in land-use regression models to predict nitrogen dioxide concentrations for health exposure studies, with some adopting remote sensing techniques (Arain et al. 2007; Knibbs et al. 2018). This inspired us to introduce spatial factors to link a scenario HIA via land-use analyzes to a post-EIA.

Here, a case of municipal sewage treatment plant (MSTP) volatile organic compounds (VOCs) is presented. Odors released from treatment units have long been a challenge when managing MSTPs (Gruchlik et al. 2017) and are naturally linked to the adopted treatment technique. MSTP odors are regarded as typical MSTP pollutants (Wang et al. 2018a, b) and generate wide concern. Here MSTP odors are taken as an example to probe HIA theory with a post-EIA. This paper addresses a way to introduce

the geographic factors of a scenario HIA via land-use to the post-EIA of an operational MSTP.

Materials and methods

Screening priority control MSTP pollutants

MSTP odors are reported widely and are classified as odors volatile pollutants, including alkanes, alkenes, aromatic hydrocarbons, halogenated hydrocarbons, sulfur-containing organic compounds, oxygenated organic compounds, hydrogen sulfide (H_2S), ammonia (NH_3), and carbon disulfide (Lewkowska et al. 2016; Liu et al. 2017). Additional odors pollutants have been confirmed as being released from grate, grit chamber, and sludge treatment units (Liang and Liu 2016; Meng et al. 2016; Ren et al. 2018). In this paper, two typical pollutants, H_2S and NH_3 , were chosen as characteristic pollutants indicating odors because neither has ever been explored at high levels, that is, H_2S levels of $145,700 \mu\text{g}/\text{m}^3$ and NH_3 levels of $63 \mu\text{g}/\text{m}^3$ (QEP et al. 2010; Lehtinen and Veijanen 2011; Wang 2013), for an extreme situation at an operational MSTP.

Meteorological parameters

The studied MSTP is located in the Haidian District of Beijing. Meteorological data from 1992 to 2016 were surveyed and used for further analyzes. Wind directions, which play an important role in pollutant diffusion predictions, were summarized. Austal 2000 G was employed to simulate the pollutant diffusion, and meteorological data of the annual 2017 parameters were adopted.

Pollutant diffusion simulations

Environmental monitoring

The environmental monitoring included both manual and online methods. The monitoring time was set to the summer because volatile odors are known to be relatively serious during this period. Manual sampling was conducted following the requirements of *China standard Air and exhaust gas monitoring and analysis methods*. The H_2S analysis followed the *China standard GB/T11742–1989*, the NH_3 analysis followed the *China standard HJ533–2009*, and the odor analysis followed the *China standard GB/T14675–93*. All the procedures, including manual sampling, monitoring, and analysis, complied strictly with quality control regulations. The manual monitoring period lasted from August 28 to 30, 2018, with a frequency of two times a day. The monitoring times were 03:00–04:00 and 16:00–17:00, avoiding rainy and windy days.

The OLFOSENSE (AIRSENSE) instrument was adopted as an online monitor; this instrument is composed of a variety of hybrid sensor arrays (four metal oxide sensors, one photo-ion detector, and four types of electrochemical sensors). The levels of the pollutants, that is, H_2S , NH_3 , and odors, were recorded by the online instruments in real time. Instantaneous data were read five times a minute, with the average value being calculated and recorded automatically. All equipment was regularly inspected and maintained in a timely manner to ensure the quality of the readings. Abnormal MSTP operating conditions may produce extreme emissions; to obtain the frequency of such extremes, we used the maximum value monitored, divided by the average annual predicted value.

Prediction of the emission source

Two situations were taken into account to evaluate the source emissions: normal and extreme conditions that are, assuming that all deodorization measures failed. The incident probabilities of an extreme condition were weighted by the accident odds for similar industries.

Pollutant diffusion simulation

The main simulated data came from the monitor results, and the diffusion variation was simulated using the AUSTAL 2000 G software. The odor time, that is, the duration of the odors, was chosen as the basic parameter. Odor levels higher than the value set as the olfactory threshold, c_{GS} , were selected by the program. The hourly average values, \bar{c} , of the selected odor parameters were calculated with a guarantee rate of more than 90%, $c_{0.9}$. When the hourly average value of $c_{0.9}$ was higher than the threshold value c_{GS} , the odor duration time of the monitored odors in that hour was recorded. That is, when the odor value $c_{0.9}$ was higher than the threshold value c_{GS} , the time in which odors were monitored in the counterpart hour was recorded as the odor duration time. In the spatial analysis, each grid from others' distance for prediction was 20 m, and the total number of grids was 200×200 . The center point coordinate was near the main odor discharge cylinder in the MSTP. The research area was designated by a geographic circle with a radius of 4 km from the center point.

Scenario exposure levels according to the land-use analysis

Exposure profile survey

The demographic characteristics and the counterpart exposure behaviors were obtained via the land-use attributes. The land-use information was obtained from the municipal land

administration. According to the information offered by the local government, the land uses in the Haidian District were classified into several types, including commercial, office, residential, school, and grassland. These classes were verified by our field investigation and data analysis. The results indicate that there were no other industries near the MSTP; however, there were some residential areas and office buildings. A grid of $20 \text{ m} \times 20 \text{ m}$ was set in the program. The population number in each land grid was counted, along with the social characteristics of the population. Similar land-use types were consolidated into a single type, and then the counterpart population's exposure behavior was investigated. To obtain the average behavioral parameters, a group of users or residents on each type of land was selected randomly to answer a questionnaire; their exposure profiles were surveyed and then employed as land-use attributes.

A total of 310 residents around the MSTP were selected randomly for the questionnaire. All questionnaires were administered on the condition that informed consent forms were signed. The questionnaire content included education, occupation, lifestyle, daily life exposure patterns, and the participant's subjective understanding of the risk of odors. The population was categorized by socioeconomic factors including stay-at-home residents, office workers, and students. The likelihood exposure times according to the demographic characteristics were summarized and assigned to counterpart land-use attributes.

Exposure levels based on the land-use analysis

Following the simulation of the spatial superimposed distribution of the pollutants, the grid center concentration was taken as the average inhalation level for that particular location. Exposure levels for different land uses were calculated following Eq. (1), a popular technique used to make inhalation exposure assessments.

$$ADD = \frac{c * IR * ET * EF * ED}{BW * AT} \quad (1)$$

Here, ADD is the daily average exposure dose; C indicates the concentration of the chemical substances in the air; IR represents the amount of respiration; ET indicates the duration of daily exposure; EF designates the frequency of exposure; ED indicates the duration of the exposure; and BW represents the local population's average weight, according to the data gathered by our investigation. The final parameter AT is the total expected exposure time.

For mixed land-use areas, the average exposure levels were estimated using Eq. (2).

$$PWEL = \frac{\sum(pi \times ci)}{\sum pi} \quad (2)$$

PWEL is the population's average exposure level, where the population refers to people with activities in a certain geographic area, which can be divided into grid numbers i on a map; p_i represents the population inside each grid and c_i indicates the average concentration of air pollutants inside each grid in units of $\mu\text{g}/\text{m}^3$ or mg/m^3 . Different types of people, categorized by their exposure patterns based on their social attributes, may experience large differences in their exposure to MSTP pollutants. To establish the PWEL values, it is important to obtain practical activity behaviors for the demographic characteristics. In our study, we attributed the social attribute types of the population on the combined gridded map because it is easy to attribute people's exposure profiles to spatial data.

Scenario health risk analysis

After assigning the exposure amount to each geographic coordinate, a scenario health risk analysis was further conducted with respect to the traditional inhaled HIA (Zhou et al. 2011); the hazard quotient (HQ) was used to describe the risk rating:

$$HQ = E/RfD,$$

where E indicates the total exposure amount and RfD indicates the reference dose. If $HQ \geq 1$, the HIA is unacceptable; otherwise, it is acceptable.

Some uncertainty factors that may contribute to variations in the health risk need to be considered. The

collected material was assumed to have an accuracy deviation of $\pm 5\%$. Different types of people, such as children, elder, and pregnant women, were assigned a health risk sensitivity scope of $\pm 5\%$. In addition, the cumulative effects of social factors (e.g., economic income and professional background) contributed an uncertainty of $\pm 10\%$. Considering the comprehensive uncertainty mentioned above in HIA, the final evaluated HIA should be adjusted such that the prediction value is $R \pm R \times 20\%$.

Statistical analyses

Statistical analyzes were performed using the SPSS 18.0 software. All the monitoring data were submitted to a Kolmogorov–Smirnov (K–S) normal distribution test. When $P > 0.05$, the data are considered to be consistent with a normal distribution. ARC GIS 10.4.1 was used to map the risk contours.

Results

Meteorological analysis

The wind direction frequency (FWD) was summarized by analyzing the meteorological data (Table 1). Due to the influence of the monsoon, the FWD varies with the season. The dominant wind direction in winter is considered to be NNE, NE, and N, with appearance frequencies of

Table 1 Statistics of frequency of wind direction (%)

Wind direction	Spring (March–May)	Summer (June–August)	Autumn (September–November)	Winter (December–February)	Annual
N	9.3	10.7	11.0	12.3	10.8
NNE	11.0	13.0	14.7	15.3	13.5
NE	9.3	11.0	13.7	13.7	11.9
ENE	3.3	3.7	3.0	2.3	3.1
E	2.0	2.7	1.7	1.3	1.9
ESE	1.0	1.7	1.0	1.0	1.2
SE	2.7	3.0	1.3	0.7	1.9
SSE	3.7	3.7	2.0	1.3	2.7
S	11.0	12.0	7.7	4.7	8.8
SSW	12.3	10.0	6.7	6.7	8.9
SW	5.3	5.7	5.0	4.3	5.1
WSW	2.0	2.3	2.0	2.0	2.1
W	2.3	2.0	2.3	2.3	2.3
WNW	2.3	1.0	2.0	2.7	2.0
NW	5.3	2.3	5.3	7.3	5.1
NNW	9.7	5.0	7.0	12.0	8.4
C(Static wind)	6.7	11.0	13.3	9.3	10.1

15.3%, 13.7%, and 12.3%, respectively. In spring, the FWD shifts to SSW and S, with frequencies of 12.3% and 11.0%, respectively, followed by NNE, with a reported frequency of 11.0%. The dominant wind direction in summer was confirmed to be NNE, NE, and N, with frequencies of 13.0%, 11.0%, and 10.7%, respectively, followed by S and SSW. Meanwhile, in autumn, the dominant wind direction was NNE, NE, and N, with frequencies of 14.7%, 13.7%, and 11.0%, respectively. With respect to the historic meteorological data, annual meteorological data including hourly data of the meteorological parameters in 2017 were set as the main meteorological parameters for the simulation, and a breeze rose diagram (Fig. 1) indicates that the wind frequency in 2017 was similar to that in previous years. In 2017, the dominant wind directions were NNE, NE, and N, with frequencies of 13.5%, 11.9%, and 10.8%, respectively, and rather low FWD values were seen for E, ESE, and SE, with frequencies of 1.9%, 1.2%, and 1.9%, respectively. Our findings suggest that the main FWDs affecting air pollutant diffusion were in the NNE and NE directions.

Contaminant diffusion simulations

To map the spatial diffusion of the pollutants, we need to obtain the emission strength and predict the diffusion according to the geographic and meteorological parameters.

Environmental monitoring

Air samples were monitored in August, when extremely hot weather conditions are ideal for VOC emissions. The hourly average levels of the pollutants were monitored (Table 2), as well as the values lower than the standard (0.01 mg/m^3). The duration of the online monitoring was from 0:00 on August 24 to 12:00 on September 2 (Fig. 2, including Figs. 2a–d). The maximum pollutant period was observed to be between 14:00 and 18:00 (Table 3). The maximum value during this period was taken assuming that the extremely risk from source emission may take place. Here, the odor concentration was estimated to be 1318 (nondimensionalize value), the H_2S emission rate was approximately $6.94 \times 10^{-5} \text{ kg/h}$, and the NH_3 emission rate was $6.75 \times 10^{-2} \text{ kg/h}$. The extreme pollution

Fig. 1 Wind rose map in 2017

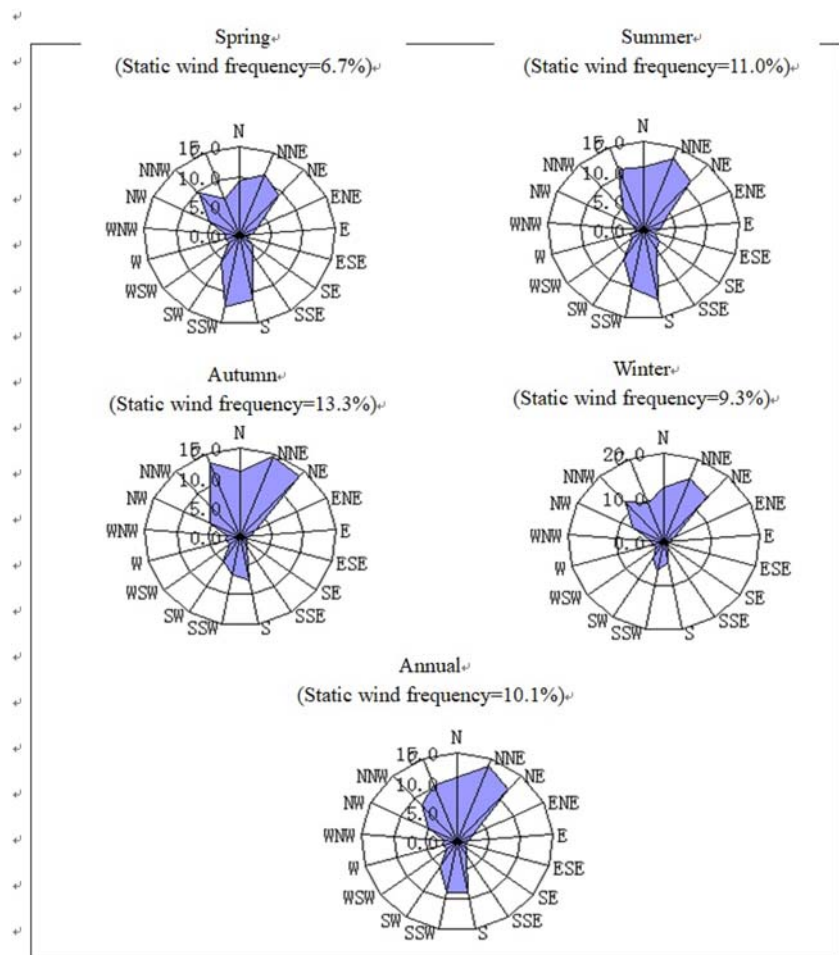


Table 2 Hourly average levels of pollutants

Pollutants	Monitor sites	Concentration (mg/m ³)	Standard limit (mg/m ³)	Concentration ratio to the standard (%)	Over-standard rate (%)
H ₂ S	1	0.005	0.01	undetected	/
	2	0.005~0.007		undetected ~70	/
	3	0.005~0.008		undetected ~80	/
	4	0.005~0.008		undetected ~80	/
NH ₃	1	0.015~0.084	0.2	7.5~42	/
	2	0.024~0.083		12~41.5	/
	3	0.012~0.086		6~43	/
	4	0.016~0.086		8~43	/
odor	1	10	10	undetected	/
	2	10		undetected	/
	3	10		undetected	/
	4	10		undetected	/

Monitor sites were set 1000 m away from the source emission. Monitor sites numbers were assigned. The east one was 1, the west one was 2, the north one was 3 and the south one was 4. The determination limits (DL) of H₂S was set as 0.005 mg/m³, as well as NH₃ and odor was 10 mg/m³. DL was replaced with the lowest level on condition that the level was lower than DL

levels were set assuming that all deodorization measures had failed; these values were assumed to be 4169 for odors, 1.96×10^{-4} kg/h for H₂S, and 1.96×10^{-2} kg/h for NH₃.

Prediction of the emission source and spatial simulation

Diffusion levels of the average annual H₂S emissions were plotted spatially (Fig. 3). The maximum was 2.8×10^{-3} μg/m³, appearing 100 m southwest of the emission source, with a

0.14% ratio to the standard value (0.01 mg/m³). The annual average H₂S levels around the spatial grids for the sensitivity subjects whereas the population was concentrated changed from 1.39×10^{-4} to 6.10×10^{-4} μg/m³ (not shown). The levels of the H₂S prediction were far lower than the standard, and the maximum H₂S value appeared southwest of the emission source. The annual average levels of NH₃ (Fig. 4) showed a diffusion trend similar to H₂S with respect to the geography (Figs. 3 and 4). The average odor levels exhibited the

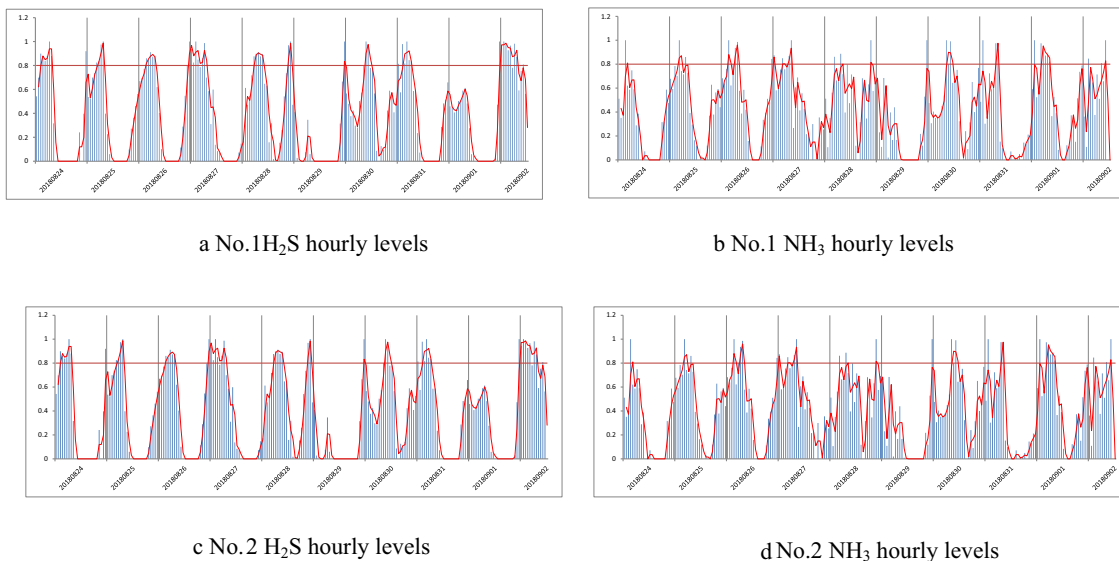


Fig. 2 Levels of H₂S and NH₃. Note: Air samples were monitored in the August, the days an extremely hot weather condition for the VOCs emission. Duration monitor online had been performing from 0:00

August 24–12:00 September 2 (a–d). The emission levels fell down to zero during the night-time because of all running chambers closed. The maximum value were chosen for the extremely scenario risk calculation

Table 3 Prediction of the emission sources

Odor factors	Normal working condition	Abnormal condition	90% working condition
Odor concentration(Dimensionless)	1318	4169	417
Hydrogen sulfide(kg/h)	6.94×10^{-5}	1.96×10^{-4}	1.96×10^{-5}
Ammonia(kg/h)	6.75×10^{-2}	0.196	1.96×10^{-2}

Note: Odor concentration was addressed in the ratio format with the detection method “Three-point comparison stinky bag method”, china standard GB/T 14675–93. By the standard, the limit value was set as 2000 on the exhaust height 15 m, and 6000 in the exhaust height 25 m

frequency of annual odor occurrences in each grid (Fig. 5). More than 4% of the high-frequency odors occurred at a distance of 1000 m from the emission source. The extreme condition revealed that odors occurred frequently around the sensitivity points, varying from levels of 3.2% to 10.8% (not shown) and at levels of more than 6% in some locations. It is suggested that the MSTP should take measures to mitigate odors and avoid occurrences of extreme conditions. The current findings, the prediction of the emission source, and the simulation on the spatial grids can be used to associate the pollutants with potentially sensitive segments of the population that may be exposed to these pollutants (Fig. 6).

Exposure parameters of sensitive populations according to the land-use analysis

Exposure parameters

Based on the land-use analysis, the main geographic grids affected by pollutant diffusion were residential estates, a kindergarten, and parts of office buildings. Other areas were grassland. Similar land-use function grids (20 m × 20 m) were combined for the spatial analysis (Fig. 6), and the counterpart population were classified into several types according to their social attributes. According to our investigation, younger

people paid more attention to MSTP risks and hazardous materials because they were better educated with respect to the potential risks of odors and were more exposed to social media than the older population. Office workers preferred to spend less time outdoors than children. Older residents mostly preferred to stay home with their windows closed. The socio-classification types of the population were sorted, and their exposure profiles are summarized in Table 4 (including 4a–4f). The behaviors of the exposure types were queried and investigated statistically; however, there was no difference on prevention odor ($p > 0.05$).

Estimation of the exposure amount

To protect the population as much as possible, the scenario emission amounts were assumed to be at the extreme condition for the following exposure evaluation. The annual exposure levels of sensitive populations (Table 5) were estimated taking into account parameters reported previously (Zhou et al. 2011; Du et al. 2014).

HIA scenarios

Next, the non-carcinogenic risk was assessed. The RfD value for the risk assessment was derived from data on the Internet

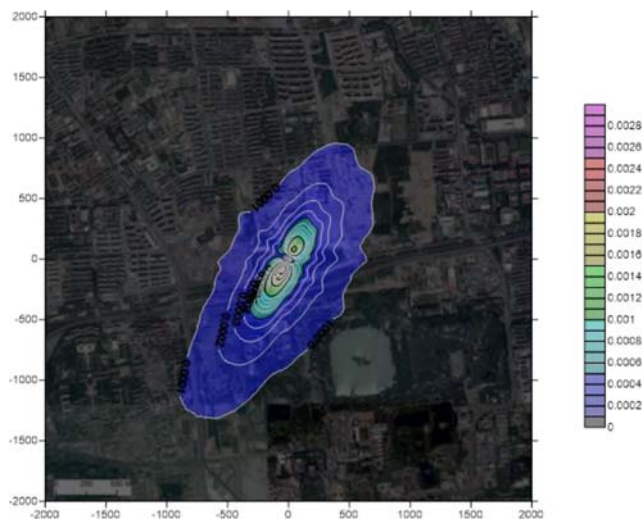


Fig. 3 Average annual H₂S concentration distribution diagram (Unit: μg/m³)

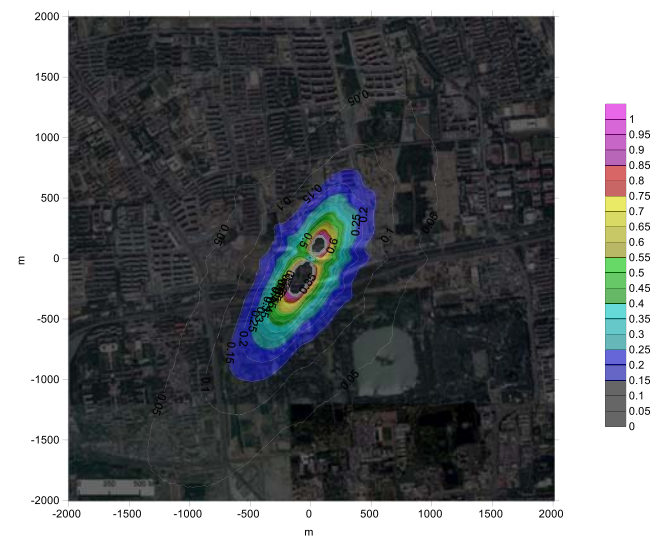


Fig. 4 Average annual NH₃ concentration distribution diagram (μg/m³)

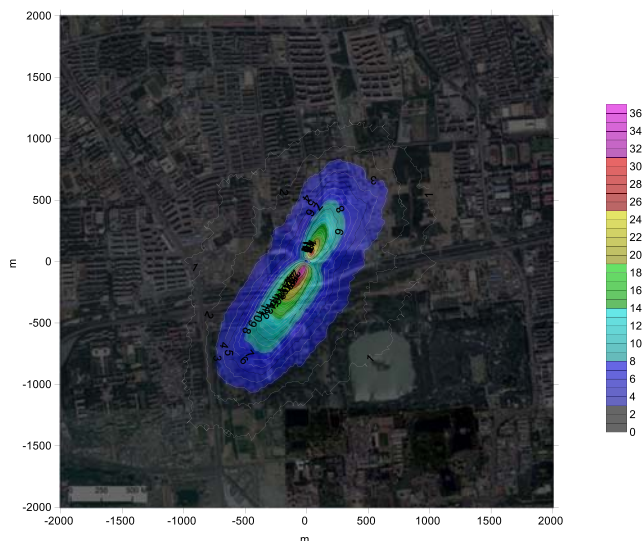


Fig. 5 Average annual odor hours frequency (Total releases 4169 OU/s, Unit: %)

(https://rais.onrl.gov/cgi-bin/tools/TOX_seaScenarioIorch?select=chem). The sub-chronic oral reference dose for H₂S was 3.00×10^{-2} mg/kg-day and the chronic oral reference dose for NH₃ was 3.40×10 mg/kg-day. The HIA contour map is displayed in Fig. 7. This map demonstrates that both the H₂S and NH₃ health risks were acceptable for all grids, even for the extreme condition, and that both odds were less than one in a hundred. Therefore, the post-EIA of the MSTP verified the security of the surrounding population. Given that uncertainty factors were taken into account, the HIA is within acceptable levels.



Fig. 6 Geographical distribution of the sensitivity people

Discussion

EIA has been successfully promoted to integrate environmental considerations into development projects. The practical applications of EIA have led to the emergence of two spin-off assessment approaches: social impact and cumulative impact assessments. Such assessments not only identify the strategic choices that might lead to more sustainable health outcomes but also reduce risks to an already operational project.

Many researchers have attempted to integrate HIA into EIA (Fehr 1999; Demidova and Cherp 2005; Bhatia 2007; Corburn and Bhatia 2007; Rajiv and Aaron 2008; Valeberg et al. 2009; Harris et al. 2015; Chanchitpricha and Bond 2018), and some have tried to employ geographic parameters to identify the scope of the health effects and the emission source sites (Johnston et al. 2019); however, a standard guideline for how to integrate HIA into EIA has not yet come into being due to academic complications with respect to this integration. The lack of HIA in EIA practices is a difficult obstacle to overcome when human health protection is concerned; however, this is less of a problem in post-EIA. The usual HIA procedure contains four steps: (1) hazard identification, (2) dose response, (3) exposure assessment, and (4) risk characterization. Exposure assessment, a crucial step in HIA, is usually performed using monitoring data with weak spatial identification (Bari and Kindzierski 2018a, b; Huang et al. 2019). The reason for the HIA deficiency in EIA in practice is the lack of a spatial factor in its overall theoretical system compared to EIA. To integrate HIA into EIA, we connected the simulation of the pollutant diffusion with the scenario population’s exposure via spatial land-use parameters. A case examining odors from an MSTP was addressed here.

Three aspects to this problem need to be considered. Traditionally, the first step involves identifying the types of adverse health effects that can be caused by exposure to the pollutants in question and characterizing the quality and weight of evidence supporting this identification. Complying with this principle, the priority control pollutants of the MSTP were weighed by their emission amounts, which are linked closely with the treatment units and techniques (Jianting et al. 2015; Lewkowska et al. 2016). H₂S and NH₃ were both chosen as characteristic pollutants indicating odors because they have both been released in large amounts, causing wide concern (Bandosz et al. 2000). Both are often produced from the microbial breakdown of organic matter by sulfate-reducing microorganisms in the absence of oxygen gas, in a process commonly known as anaerobic digestion. These gases can cause an unpleasant smell and produce long-term adverse effects.

The second problem relates to defining the dose–response parameters. Usually, for available toxic dose–response parameters that have been approved and deduced by previous

Table 4 The exposure profiles were summarized

a. People exposure profiles on spatial						
Crowd sensitive target	Distance(m)	Population socail type				
Qicaihuayuan village	490	Mixed				
Summer Palace Garden Villa’s	510	Mixed				
Geracomium	410	Elderly				
Kindergarten	490	Children				
Destruction center	490	Mixed				
Xiaojiahe village	610	Mixed				
Shu vilage	550	Mixed				
Plain white banner Vilage	950	Mixed				
Fengzeyinghe village	900	Mixed				
Wanshu village	950	Mixed				
Malianwajuyuan	1950	Mixed				
Malianwazhuyuan	1950	Mixed				
Boya village	840	Mixed				
Shangdi west village	1700	Mixed				
Shangdi east village	2100	Mixed				
b. Exposure parameters of residential adult inhalation						
Residence adult	IR m ³ /d	ET h/d	EF d/a	ED 年	BW kg	AT d/years×365
Male	18.65	1	292	40	67.78	40 × 365
Female	14.93	1	292	40	59.00	40 × 365
Avg.	16.79	1	292	40	63.39	40 × 365
c. Exposure parameters of children (<6 years old)						
Residence Children	IR m ³ /d	ET h/d	EF d/a	ED 年	BW kg	AT d/years×365
Avg.	5.6	0.33	237	10	16.61	10 × 365
d. Exposure parameters of old man (>60 years old)						
Residence Elder	IR m ³ /d	ET h/d	EF d/a	ED 年	BW kg	AT d/years×365
Avg.	13.24	1	365	30	60.28	30 × 365
e. Exposure parameters of students (>12 years old)						
Residence Student	IR m ³ /d	ET h/d	EF d/a	ED 年	BW kg	AT d/years×365
Avg.	14.65	0.5	365	70	59.65	70 × 365
f. Exposure parameters of office man						
Residence Office worker	IR m ³ /d	ET h/d	EF d/a	ED 年	BW kg	AT d/years×365
Avg.	16.79	0.5	292	40	63.39	40 × 365

For those mixed types of residential adults live surrounding, exposure amount were set as the scenario extremely exposure to MSTP, with the daily exposure time 24 h, the exposure frequency was estimated as 80% of the annual, and thus, the EF was set as 292 days, while the duration lifetime was 40 years

Table 5 Estimation of the sensitivity people’s average exposure amount

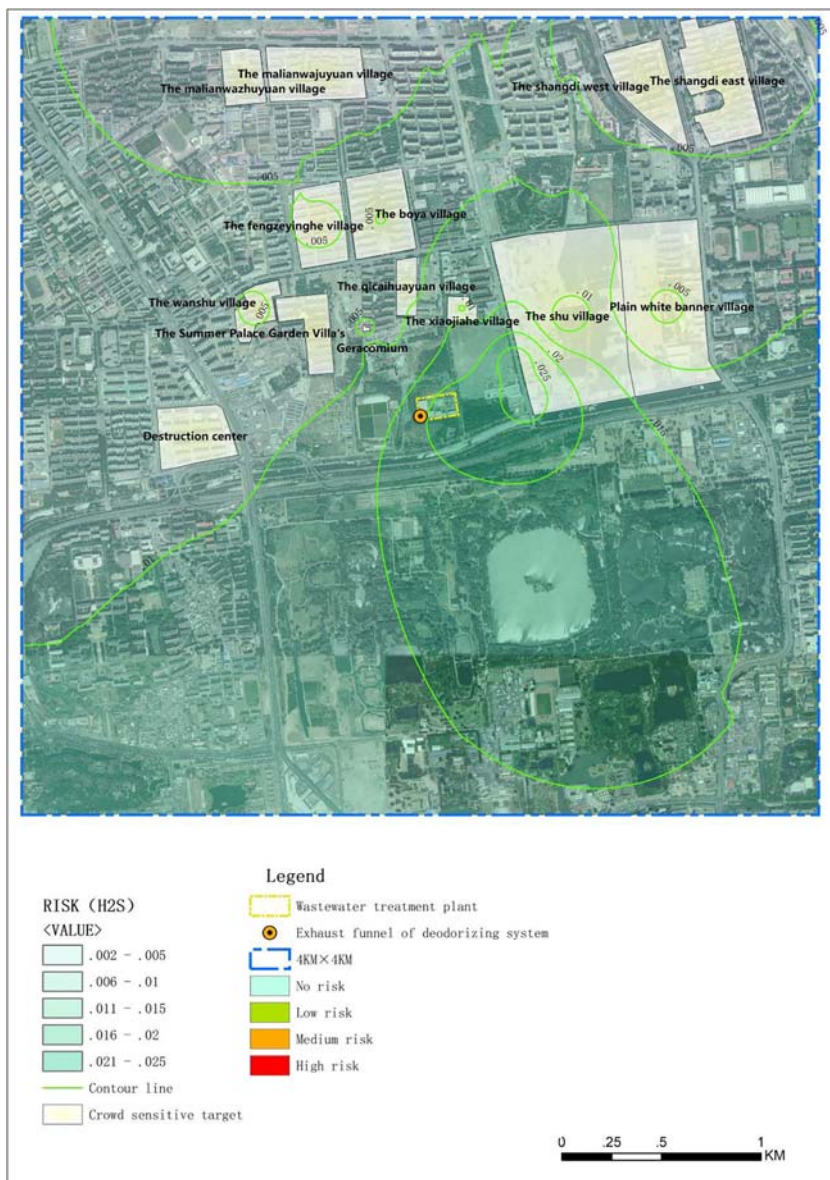
Sensitive crowd	H ₂ S(μg/m ³)	NH ₃ (μg/m ³)
Qicaihuayuan village	0.131	3.51
Summer Palace Garden Villa’s	0.126	3.38
Geracomium	0.154	4.11
Kindergarten	0.131	3.51
Destruction center	0.131	3.51
Xiaojiahe village	0.104	2.78
Shu village	0.116	3.12
Plain white banner village	0.059	1.59
Fengzeyinghe village	0.068	1.81
Wanshu village	0.064	1.71
Malianwajuyuan village	0.059	1.59
Malianwazhuyuan village	0.023	0.61
Boya village	0.023	0.61
Shangdi west village	0.070	1.87
Shangdi east village	0.027	0.73

studies, the dose–response parameters can be cited directly. In this study, a sub-chronic oral reference dose of H₂S of 3.00 × 10⁻² mg/kg-day and a chronic oral reference dose of NH₃ of 3.40 × 10 mg/kg-day were used.

The third aspect deals with how to conduct exposure assessments by incorporating spatial factors into the HIA theory, the most important procedure to incorporate HIA into post-EIA. Two aspects need to be coordinated using the same geographic factors. First, the diffused contaminants need to be obtained based on the geography, and then the exposure amount, which is linked closely with the population’s exposure profiles on the counterpart lands, needs to be estimated. People’s activities, which are determined by their social characteristics, are correlated closely with the land-use areas in which they are located.

Meteorological parameters are critical factors in the contaminant diffusion simulation. In our study, historic FWD statistics were analyzed (Table 1) and used to evaluate the main wind directions in the prediction. The dominant historic wind

Fig. 7 Contour map of HRA



directions were NNE, NE, and N, with frequencies of 13.5%, 11.9%, and 10.8%, respectively, in keeping with the annual meteorological parameters for 2017, the trends of which are shown on a wind rose map (Fig. 1). The results indicate that the main wind directions affecting the air pollutant diffusion were NNE and NE.

In general, pollutants released from the MSTP during normal conditions need to be known, and while assessing HIA, the abnormal condition in which all deodorization measures failed should be taken into account.

The monitoring of the hourly average pollutant levels via manual sampling was performed (Table 2) and indicated that all results were lower than the standard (0.01 mg/m³). The maximum values were defined as the top values from the online duration monitor (Fig. 2), which had a fluctuating

scope. That is, the extreme risk was assumed at the maximum value. The predictions of the emission source contained both conditions (Table 3). The extreme odor level was 4169, and the emission rates for H₂S and NH₃ were 1.96×10^{-4} and 1.96×10^{-2} kg/h, respectively. The extreme HIA health risk scenario was based on the conditions necessary to eliminate most of the health risk.

More challenging techniques were employed to develop the spatial HIA. The spatial variations in the pollutant diffusion were simulated using Austal 2000 G (Figs. 3, 4, and 5). All pollutant distributions had trends similar to the FWD (Fig. 1). The maximum annual average of H₂S concentration was found to be 2.8×10^{-3} µg/m³, appearing southwest of the emission source with a 0.14% ratio to the standard (0.01 mg/m³). This finding implies that this area is of primary concern.

A further analysis revealed that the annual average H₂S level around the sensitive points where the population was concentrated changed from 1.39×10^{-4} to 6.10×10^{-4} $\mu\text{g}/\text{m}^3$. Our results indicate that the predicted H₂S level was far lower than the standard and the maximum levels southwest of the emission source. However, both H₂S and NH₃ had the same trends as the odors, and the meteorological data played an important role in their diffusion. The dependency of the diffusion conditions of the air pollutants on the meteorological parameters is supported by previous studies (Ilten and Selici 2008; Sabetghadam and Ahmadigivi 2014).

Based on the diffusion map (Figs. 3, 4, and 5), the land uses in each grid were investigated. Crowded areas were defined as sensitive points, and the geographic distribution of their coordinates was surveyed (Fig. 6); most residents are located north of the emission source in the upwind direction. Subsequently, similar land-use grids were merged. Most areas were classified as living areas, residential houses, elderly care centers, offices, and a kindergarten. Other areas were designated as grassland. Population classes and exposure profiles were summarized based on the land-use (Table 4). Mixed buildings indicated the presence of different social types of people in the same building, including office workers, retired individuals, and students. Multi-function buildings were composed of accommodations and business offices. The behaviors of the exposure types were further queried, and the results indicate that there is no difference on prevention odor ($p > 0.05$). The younger generation paid more attention to the risks of the MSTP. It is important to define a timeframe for HIA, and all lifetimes were set to 70 years. Combined with the exposure parameters reported previously (Bai et al. 2007; Huang et al. 2017), the annual exposure amounts of the sensitive populations were calculated (Table 5) assuming the extreme condition.

In the final step, the spatial risk scenario characterizations provided a risk appraisal calculated on the basis of the exposure and hazard. An HIA contour map was created accordingly, showing the spatial factors linking HIA to the pollutant diffusion (Fig. 7). This map summarizes the information integrated from the proceeding steps of the risk assessment, making it easy to assess the HIA spatially. In this case, both the H₂S and NH₃ health risk levels were acceptable on all grids, even for the extreme condition. Including the uncertainty factors, the HIA is still at an acceptable level. Therefore, the HIA of H₂S and NH₃ for the MSTP post-EIA indicated that the surrounding population is not in danger.

In this paper, we proposed a systematic and thorough approach to connect HIA with post-EIA and to motivate the integration of HIA into post-EIA using the case of an MSTP. This approach will provide environmental evidence to support decision-making related to the protection of human health.

Conclusions

Human health protection is considered to be a major target of EIA, by both decision-makers and the public. However, in current operational projects, human health protection is constrained by the lack of techniques for post-EIAs. This paper presents an approach to develop an HIA scenario for post-EIA systems by introducing a spatial factor including the spatial diffusion of pollutants and the population's activity characteristics based on land-use at the geographic scale. A specific case, the linkage of HIA to the EIA of an MSTP, was discussed here, addressing an approach to resolve the lack of HIA in the current EIA. It is important to complete EIA theory and to promote the most conducive strategy to enhance human health protection and reduce negative impacts. Further theoretical and practical studies still need to be conducted.

Acknowledgments The authors are extremely grateful to the staff at the Department of Environment and Health for their health statistics technical guides. The findings and conclusions in this report are those of the authors. The authors declare that they have no competing financial interests.

Authors' information Not applicable.

Authors' contributions The authors' responsibilities were as follows—Hongmei Wang is the PI of the parent project and obtained funding and supervised all scientific aspects of the work; Huifeng Wang, Ci zhao, Xiang Huang, and Zhanlu Lv formulated the research questions and designed the study and mediation analysis; Xiaoyu liu designed data protocols and collected data; Xiang Huang provided essential materials; Ci zhao handled all statistical programming and analysis; Zhanlu Lv interpreted results; Hongmei Wang wrote the paper; Hongmei Wang had primary responsibility for final content. All authors read and approved the final manuscript.

Funding information The research presented here was supported by Chinese Ministry of Science and Technology Project 2018YFC0213704.

Availability of supporting data Not applicable.

Compliance with ethical standards

Consent for publication Not applicable.

Ethical approval and consent to participate No applicable.

Competing interests The authors declare that they have no competing interests.

References

- Aliyu AS, Ramli AT, Saleh MA (2014) Environmental impact assessment of a new nuclear power plant (NPP) based on atmospheric dispersion modeling. *Stoch Env Res Risk A* 28(7):1897–1911
- Arain MA, Blair R, Finkelstein N, Brook JR, Sahsuvaroglu T, Beckerman B, Zhang L, Jerrett M (2007) The use of wind fields in a land use

- regression model to predict air pollution concentrations for health exposure studies. *Atmos Environ* 41(16):3453–3464
- Bai Z, Hu Y, Yu H, Wu N, Ding X, Zhu T (2007) Health risk assessment on citizens of inhalation exposure to environmental PAHs in Tianjin, China. international symposium on ambient air particulate matter: techniques and policies for pollution prevention and control
- Bandosz TJ, Bagreev A, Adib AF, Turk A (2000) Unmodified versus caustics-impregnated carbons for control of hydrogen sulfide emissions from sewage treatment plants. *Environ Sci Technol* 34(6):1069–1074
- Bari MA, Kindziński WB (2018a) Ambient volatile organic compounds (VOCs) in Calgary, Alberta: sources and screening health risk assessment. *Environmental Pollution* 631–632:602–614
- Bari MA, Kindziński WB (2018b) Ambient volatile organic compounds (VOCs) in Calgary, Alberta: sources and screening health risk assessment. *Sci Total Environ* 631–632:627–640
- Bhatia R (2007) Protecting health using an environmental impact assessment: a case study of San Francisco land use decisionmaking. *Am J Public Health* 97(3):406–413
- Boudet C, Zmirou D, Laffond M, Balducci F, Benoit-Guyod J-L (1999) Health Risk Assessment of a Modern Municipal Waste Incinerator. *Risk Anal* 19(6):1215–1222
- Chanchitpricha C, Bond A (2018) Investigating the effectiveness of mandatory integration of health impact assessment within environmental impact assessment (EIA): a case study of Thailand. *Impact Assess Proj Apprais* 36(1):16–31
- Chang IS, Yilihamu Q, Jing W, Wu H, Bo N (2017) Health impact assessment in environmental impact assessment in China: status, practice and problems. *Environ Impact Assess Rev* 66:127–137
- Corburn J, Bhatia R (2007) Health impact assessment in San Francisco: incorporating the social determinants of health into environmental planning. *J Environ Plan Manag* 50(3):323–341
- Demidova O, Cherp A (2005) Risk assessment for improved treatment of health considerations in EIA. *Environ Impact Assess Rev* 25(4):411–429
- Du Z, Mo J, Zhang Y (2014) Risk assessment of population inhalation exposure to volatile organic compounds and carbonyls in urban China. *Environ Int* 73:33–45
- Fehr R (1999) Environmental health impact assessment: evaluation of a ten-step model. *Epidemiology* 10(5):618–625
- Gruchlik Y, Fouché L, Joll CA, Heitz A (2017) Use of alum for odor reduction in sludge and biosolids from different wastewater treatment processes. *Water Environ Res* 89(12):2103–2112
- Harris P, Viliani F, Spickett J (2015) Assessing health impacts within environmental impact assessments: an opportunity for public health globally which must not remain missed. *Int J Environ Res Public Health* 12(1):1044–1049
- Huang Y, Du W, Chen Y, Shen G, Su S, Lin N, Shen H, Zhu D, Yuan C, Duan Y (2017) Household air pollution and personal inhalation exposure to particles (TSP/PM_{2.5}/PM_{1.0}/PM_{0.25}) in rural Shanxi, North China. *Environ Pollut* 231(Pt 1):635–643
- Huang H, Lin C, Yu R, Yan Y, Li H (2019) Contamination assessment, source apportionment and health risk assessment of heavy metals in paddy soils of Jiulong River basin, Southeast China. *RSC Adv* 9(26):14736–14744
- Ilten N, Selici AT (2008) Investigating the impacts of some meteorological parameters on air pollution in Balıkesir, Turkey. *Environ Monit Assess* 140(1–3):267–277
- Jianting YI, Zhang C, Feng XU, Luo C, Chen H, Zhao X (2015) The status and developing trend of municipal sewage treatment plants in China. *Environmental Chemistry*
- Johnston L, Davison C, Lkhagvasuren O, Janes CR (2019) Assessing the effects of a Canadian-Mongolian capacity building program for health and environmental impact assessment in the mining sector. *Environ Impact Assess Rev* 76:61–68
- Knibbs LD, Coorey CP, Bechle MJ, Marshall JD, Hewson MG, Jalaludin B, Morgan GG, Barnett AG (2018) Long-term nitrogen dioxide exposure assessment using back-extrapolation of satellite-based land-use regression models for Australia. *Environ Res* 163:16
- Lamoreaux J, Arizona UO (2019) “Swimming in poison”: reimagining endocrine disruption through China’s environmental hormones. *Cross-Currents: East Asian History and Culture Review* 8
- Lebret E (2015) Integrated environmental health impact assessment for risk governance purposes; across what do we integrate? *Int J Environ Res Public Health* 13(2):71
- Lehtinen J, Veijanen A (2011) Determination of odorous VOCs and the risk of occupational exposure to airborne compounds at the waste water treatment plants. *Water Sci Technol* 63(10):2183–2192
- Lei L, Hilton B (2012) Designing a Spatially Intelligent Framework to Improve Public Participation in the EIA Process for Renewable Energy and Power Transmission Projects. *International Journal of Geo-Information* 2(2):480–506
- Lewkowska P, Cieślak B, Dymerski T, Konieczka P, Namieśnik J (2016) Characteristics of odors emitted from municipal wastewater treatment plant and methods for their identification and deodorization techniques. *Environ Res* 151:573–586
- Liang K, Liu J (2016) Understanding the distribution, degradation and fate of organophosphate esters in an advanced municipal sewage treatment plant based on mass flow and mass balance analysis. *Sci Total Environ* 544:262–270
- Liu C, Yang P, Liu X, Tang H (2017) Simulation analysis on odor dissipation and distribution characteristics of underground sewage treatment plant. *Refrigeration and Air-Conditioning* 17(1):79–87
- Meng X, Venkatesan AK, Ni Y, Steele JC, Wu L, Bignert A, Bergman Å, Halden RU (2016) Organic contaminants in Chinese sewage sludge: a meta-analysis of the literature of the past 30 years. *Environ Sci Technol* 50(11):5454–5466
- Minolfi G, Albanese S, Lima A, Tarvainen T, Rezza C, Vivo BD (2018) Human health risk assessment in Avellino-Salerno metropolitan areas, Campania region, Italy. *J Geochem Explor* 195:97–105
- Niu Y, Chen R, Kan H (2017) Air pollution, disease burden, and health economic loss in China. *Adv Exp Med Biol* 1017:233–242
- QEP, C. D. C. P. E, Victor JGPE, Ray HPE, Mark KPE, Neil WPE (2010) Odor investigation and control at a WWTP in orange county, Florida. *Environ Prog Sustain Energy* 20(3):133–143
- Rajiv B, Aaron W (2008) Integrating human health into environmental impact assessment: an unrealized opportunity for environmental health and justice. *Environ Health Perspect* 116(8):991–1000
- Ren B, Zhao Y, Lyczko N, Nzihou A (2018) Current status and outlook of odor removal Technologies in Wastewater Treatment Plant. *Waste Biomass Valor*:1–16
- Rouéle GA, Jabot F (2018) Health impact assessment on urban development projects in France: finding pathways to fit practice to context. *Glob Health Promot* 24(2):25
- Ruby MV, Schoof R, Brattin W, Goldade M, Post G, Harnois M, Mosby DE, Casteel SW, Berti W, Carpenter M (1999) Advances in evaluating the Oral bioavailability of inorganics in soil for use in human health risk assessment. *Environ Sci Technol* 33(21):3697–3705
- Sabetghadam S, Ahmadigivi F (2014) Relationship of extinction coefficient, air pollution, and meteorological parameters in an urban area during 2007 to 2009. *Environ Sci Pollut Res Int* 21(1):538–547
- Spickett J, Katscherian D, Goh YM (2012) A new approach to criteria for health risk assessment. *Environ Impact Assess Rev* 32(1):118–122
- Valeberg BT, Hanestad BR, Klepstad P, Miaskowski C, Moum T, Rustøen T (2009) Human health and wellbeing in EIAs in New South Wales, Australia: auditing health impacts within environmental assessments of major projects. *Environ Impact Assess Rev* 29(5):310–318
- Vu VH, Le XQ, Pham NH, Hens L (2013) Application of GIS and modelling in health risk assessment for urban road mobility. *Environ Sci Pollut Res* 20(8):5138–5149

- Wang Z (2013) Characteristics and simulation of hydrogen sulfide emission in a municipal wastewater treatment plant. (in chinese). Tsinghua University Press, Beijing
- Wang H, Lv S, Diao Z, Wang B, Zhang H, Yu C (2018a) Study on sandstorm PM 10 exposure assessment in the large-scale region: a case study in Inner Mongolia. *Environ Sci Pollut Res Int* 25(17): 17144–17155
- Wang J, Tian Z, Huo Y, Yang M, Zheng X, Zhang Y (2018b) Monitoring of 943 organic micropollutants in wastewater from municipal wastewater treatment plants with secondary and advanced treatment processes. *J Environ Sci* 67(5):309–317
- Zhou J, You Y, Bai Z, Hu Y, Zhang J, Zhang N (2011) Health risk assessment of personal inhalation exposure to volatile organic compounds in Tianjin, China. *Sci Total Environ* 409(3):452–459

Publisher's note Springer Nature remains neutral with regard to jurisdictional claims in published maps and institutional affiliations.